MECHANIKA TEORETYCZNA
I STOSOWANA
Journal of Theoretical
and Applied Mechanics
3, 35, 1997

COMPARATIVE ANALYSIS OF DYNAMIC REACTION FORCES FOR DIFFERENT TRAM VEHICLE CARRIAGE SYSTEMS IN ON-CURVE MOTION

EDMUND WITTBRODT

KRZYSZTOF LIPIŃSKI

Nazwa Instytutu lub Wydziału, Technical University of Gdańsk

e-mail: ewittbro@pg.gda.pl; klipinsk@pg.gda.pl

Multibody system dynamics formulas are well-known tools for robot dynamics examination. Concurrently they can be used to predict dynamics of road vehicles, too. Nevertheless, the multibody dynamics method is still calling for new applications. A rail transport, especially the tram transportation, which is a very popular element of mass urban transport, can be seen as a very interesting application. It should be emphasised that in comparison with trains or underground, the tram vehicles work conditions are restrained by a larger number of outside limitations. There is some literature about the rail transportation dynamics available. However, the majority of it is devoted to the behaviour characteristic for trains. In the present paper a dynamic analysis of the railway vehicles bogies, under conditions characteristic for the urban transportation is carried out. Calculation methods for various bogie types have been discussed. A special attention has been paid to the problem of choosing an appropriate dynamic model and a model of wheel-rail contact reactions. Behaviour of the bogies entering a curve of a small radius has been studied. The bogie classification criterion was the wheel-rail contact interactions; the aim was to find a bogie with the smallest actions on the rail. The results of computer simulation allowed us to identify the basic physical phenomena affecting the rail and the wheel and to assess analysed constructional designs.

Key words: dynamics, railway, tram

1. Introduction

Multibody system dynamics formulas are well-known tools for robot dynamics examination. Concurrently, they can be used to predict dynamics of road vehicles, too. Nevertheless, after equipping it with numerical tools, multibody

system dynamics method is still calling for new applications. These applications, well rooted in everyday life, are especially interesting. To deal with these new problems, a redefinition of general multibody dynamics methods is indispensable, as well as new interaction models.

The tram transport is a very popular element of the municipal transportation. Trams are seen on the streets of many cities. These vehicles are widely appreciated because of such features as a possibility of carrying a great number of passengers, or using the kind of energy that does not pollute the city environment. In comparison to trains or underground, tram vehicles work under the conditions of a much higher number of outside limitations imposed by the rules and regulations by which cities live. Reduction of the limitations is extremely difficult and expensive. Among the most important limitations are: a great number of rail-track curves, small radiuses of the curves, impossibility of rail inclination on the curves, limited possibility of introducing coaches that would deviate from the vertical position by large roll deflections, great speed on the curves, aiming at maximum efficiency at boarding and getting out of passengers, bad condition of tracks, and high requirements for the comfort of travelling.

At present, there are many works (cf Kisilowski et al., 1991; Garg and Dukkipati, 1984; Fisette and Samin, 1991) dealing with rail transportations. Unfortunately, most of them concern the train transportation, that is the kind of transportation that does not have to face the limitations mentioned above. As a result, the conclusions drawn in literature are often of no use to constructors of tram bogies. In the present study we have decided to analyse dynamic behaviour of various kinds of bogies, taking into consideration their behaviour on tram tracks.

2. The considered designs and models of appearing phenomena

The analysis will be limited to the phenomena affecting the bogies. This approach will allow us to eliminate from the model all these constructional elements that do not have a direct influence on the features of the bogie. The analysed model will be limited to two elements (Fig.1): the front car and the bogie. Then, three kinds of bogies will be examined. They can move on the following configurations of wheels:

a) blocked with a common axis in the so-called wheelset (here it will be given a symbol BW – Bogie moving on Wheelsets),

b) placed independently on a common axis (BI – Bogie moving on Independent wheels),

c) independent on separate axes of varied set geometry (BA – Bogie Articulated).

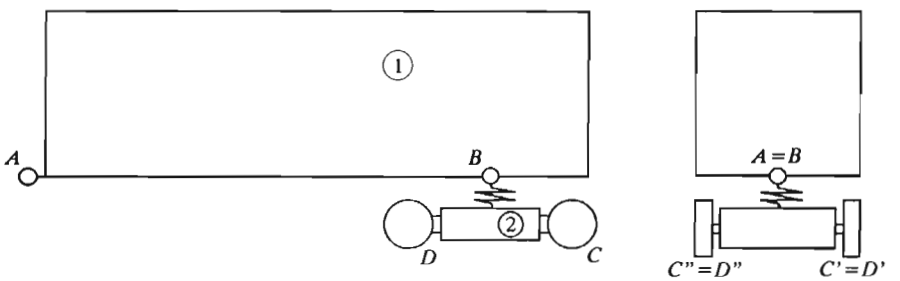

Fig. 1. Basic elements of the model: 1 – coach, 2 – bogie

2.1. Model of the front coach subsystem

The front coach model is the independent, ideally rigid body (1) of a given mass and mass moments of inertia (Fig.1). The element that links the coach with the rest of the tram is treated here as a massless and dimensionless body A. This element moves at a constant speed along the trajectory showing the central line of the track. It is connected to the coach (1) by a joint of three rotating degrees of freedom. Additionally, the coach (1) is connected to the bogie (2) at the point B by a six degrees of freedom spring and a set of three dampers arranged in a configuration characteristic for a given bogie construction.

2.2. Models of a bogie on a wheelset and on independent wheels

In view of the constructional compatibility between BW and BA designs, both types will be described here simultaneously. Each of them consists of (Fig.2):

- frame of the carriage (1),
- front-wheels axis (2) and back-wheels axis (3),
- two wheels (4) on each axis.

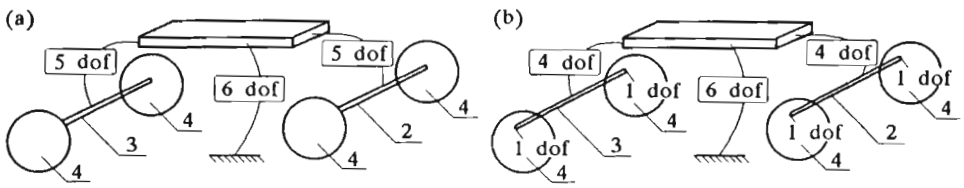

Fig. 2. Graphic representation of the model elements and the elements interconnecting the bogie with: (a) wheelsets, (b) independent wheels

The frame of the bogie has six degrees of freedom (dof): three translational and three rotational ones. The bearing of the wheel axis is interconnected with the bogie frame over the four degrees of freedom joint. Defining the longitudinal direction as collinear with the direction of the tram motion, we can assume that in the analysed joint the longitudinal direction as well as rotation around the axis are blocked. In all the other directions there are dumping and elastic elements working and generating forces or torques in case of their deformation.

In the BW bogie the axes are placed freely in the bearing, so an additional fifth degree of freedom is placed in the previously described joint and the wheels are connected with a common axis. In the BI bogie the axes are locked in the bearing and the wheels are connected to the axis by rotary motion. The models described above, represent bogies located free in space. To indicate that the bogies are located on a rail track, a set of four constrain equations is additionally introduced. The equations describe mathematically the fact that all the wheel profiles are in permanent contact with the rail profiles.

2.3. Model of an articulated bogie

An example of an articulated bogie is the bogie of BAS2000 type (Fig.3) produced by Bombardier-Eurorail BN in Belgium. The model designed for this configuration shows a mechanism used in this bogie which changes the set geometry of wheels (Fig.4). As we have found, the BAS2000 is a complex mechanical structure. To build a numerical model of it, well developed multibody formalism is necessary (cf Fisette et al., 1996).

The initial multibody structure of the bogie is composed of 13 bodies (Fig.5a). The body No. 1, which represents the bogie frame, has six degrees of freedom. All the other bodies are connected with one another by joints introducing one or two relative degrees of freedom. One degree of freedom

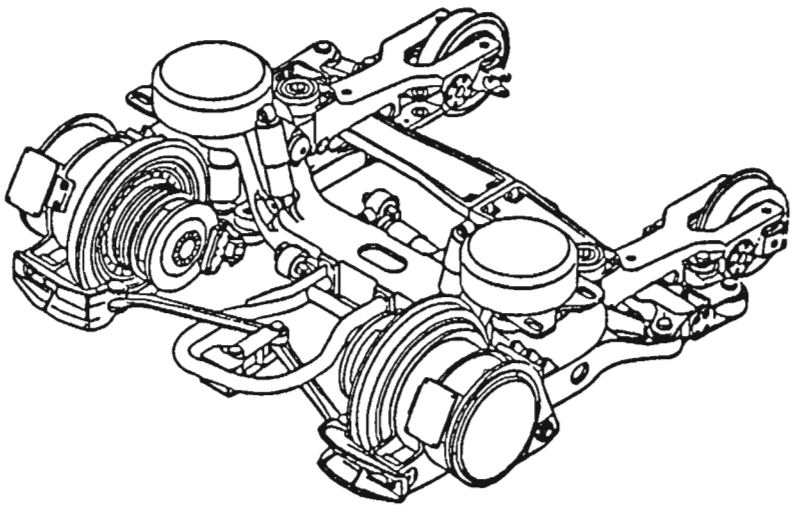

Fig. 3. Bogie BAS2000

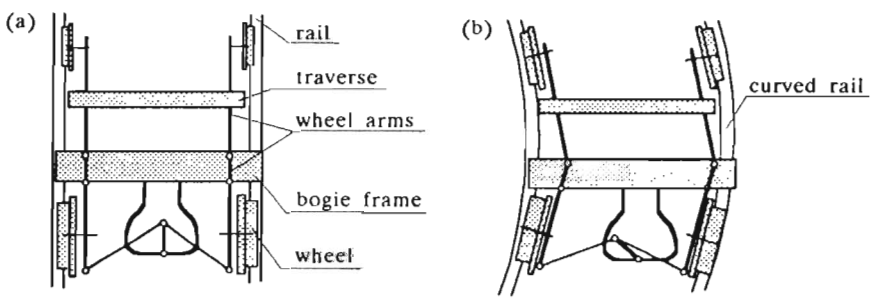

Fig. 4. BA bogie configuration; straight line (a), curve (b)

joints are presented in Fig.5a as short arcs. All two degree of freedom joints are presented as the arcs containing a dot. Additionally, in the model which does not include any closed loop of bodies, five constrains of the "cr – connecting rod" type have been introduced, together with one constrain of the "sa – spherical articulation" type (Fig.5b). Finally, motion limitations which come from the wheel-rail contact have been introduced as an additional set of four constrain equations. After considering all the constrains introduced in the configuration, the analysed mechanism has got eight degrees of freedom: six describing the position of the bogie frame in space, and two describing the changes in the set geometry of the wheels.

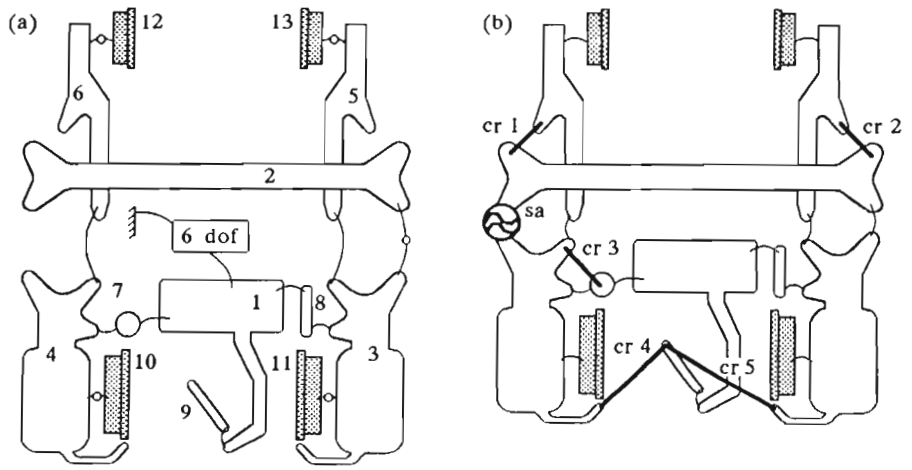

Fig. 5. Graph representation of the initial multibody structure of BAS2000 (a) and the constrains imposed on it (b)

2.4. Models of the phenomena appearring between the rail and the wheel

2.4.1. Main point of contact

At the point of contact of the wheel with the rail a considerable normal force appears. At such loads we can no longer presume that the wheel and the rail remain rigid bodies at the contact point. The analysed wheel rolls along the rail. Additionally, it moves along the arch of the route. To keep balance, a great centripetal force is needed. The friction forces appearing at main points of the contact of the wheel with the rail are often not strong enough to balance the centrifugal force, so the wheels have got special flanges to prevent them from sliding off the rail.

The contact friction forces appearing on the rolling surfaces are accompanied by slip. To describe the slip between the wheel and rail, a concept of non-dimensional creep was introduced by Carter (1926). Pointing to the fact that the rail is considered as stationary, we can use the creep concept in the notation proposed by Garg and Dukkipati (1984)

– for longitudinal creep

$$\xi_x = \frac{v_{wa} - v_{wr}}{v_{wr}} \tag{2.1a}$$

– for lateral creep

$$\xi_y = \frac{v_{pa} - v_{pr}}{v_{wr}} \tag{2.1b}$$

– for spin creep

$$\xi_{sp} = \frac{\omega_{1n} - \omega_{2n}}{v_{wr}} \tag{2.1c}$$

where

v_{wa}, v_{pa} – actual longitudinal and lateral velocities, respectively, of the rolling body

v_{wr}, v_{pr} – pure longitudinal and lateral velocities, respectively, due to the rotation of the body

ω_{in} – i-th body angular velocity component which is parallel to the normal to the contact surface of bodies.

In modelling the contact forces between the wheel and the rail, the three-dimensional linear contact theory was developed by Kalker (1967). In the general contact theory of rotating bodies we state that the contact surface between the rolling bodies is divided into two distinct regions: adhesion area with static friction forces and slip area with kinematic friction.

In the linear theory we take for granted the fact that for very small creep ξ_x, ξ_y, ξ_{sp} the slip area is so small that its influence can be neglected. It is equivalent to the assumption that in the whole contact area we deal with a deflection zone without slip. If both rolling elements are made of steel, the relations between friction forces and creep, worked out by Kalker (1967), are the following (cf Kalker, 1990)

$$\begin{aligned} F_x &= -c^2 G C_{11} \xi_x \\ F_y &= -c^2 G C_{22} \xi_y - c^3 G C_{23} \xi_{sp} \\ M_z &= -c^2 G C_{32} \xi_y - c^4 G C_{33} \xi_{sp} \end{aligned} \tag{2.2}$$

where: $c = \sqrt{ab}$, a, b are the axes of the contact ellipse (cf Hertz, 1895), G is the steel shear modulus of rigidity, C_{11}, C_{22}, C_{23}, C_{32}, C_{33} the coefficients of creep and spin (collected and presented aby Kalker (1979) and (1990)) and $C_{32} = -C_{23}$.

For more considerable creep, the approximate, non-linear method of calculating tangent forces, proposed by White et al. (1978), has been used. In this method the tangent forces are first assessed, using the Kalker linear theory, and then the expression

$$F'_R = \sqrt{F_x^2 + F_y^2} \tag{2.3}$$

is calculated. Next, taking into consideration a non-linear effect connected with the existence of friction, we will approximate the friction force by the

function (cf Garg and Dukkipati, 1984)

$$F_R = \begin{cases} fN\left[\frac{F'_R}{fN} - \frac{1}{3}\left(\frac{F'_R}{fN}\right)^2 + \frac{1}{27}\left(\frac{F'_R}{fN}\right)^3\right] & \text{for} \quad F'_R \leq 3fN \\ fN & \text{for} \quad F'_R > 3fN \end{cases} \tag{2.4}$$

To assess the components of the friction force it is necessary to determinecalculate the direction of this force. The angle between the tangent force and longitudinal direction can be calculated as:
– for small creep

$$\theta_1 = \arctan \frac{F_x}{F_y} \tag{2.5a}$$

– for considerable creep

$$\theta_2 = \arctan \frac{\xi_x}{\xi_y} \tag{2.5b}$$

For others creepage values White et al. (1978) proposed the use of a linear approximation of the angle θ. Then, for assessing the components of the tangent force, the following equations (cf Garg and Dukkipati, 1984)

$$F_{xN} = F_R \sin\theta \qquad F_{yN} = F_R \cos\theta \tag{2.6}$$

are true.

2.4.2. Point between the flange of wheel and the rail

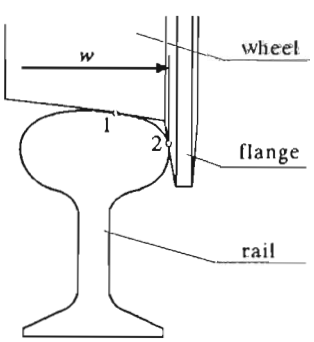

Fig. 6. Flange contact

It is well-known that rail vehicles have not got any active driving devices. To substitute this deficiency, all their wheels have been equipped with flanges (Fig.6). Then, the flange of a bogie wheel eliminates the possibility of its

transverse movement. When a danger that the wheel slipping off the rail appears, a force appears on the flange, that exerts pressure on the rail and keeps the wheel on it. Among the rail vehicles it is the tram that works under most difficult conditions. High security is required, as well as bad track condition can be expected. Simultaneously, small curve radiuses are popular. Then, to increase the vehicle security, rails can be equipped with a groove (Fig.7). The presence of groove requires modelling of a eventual point of contact on the inner and on the outward side of the flange. To model the flange contact two hypotheses are accepted:

1. The lateral position w of the contact point on the flange profile is supposed to fixed (Fig.6)

2. The second contact occurs only if the lateral displacement of the "candidate" contact point is greater that the fixed constant value.

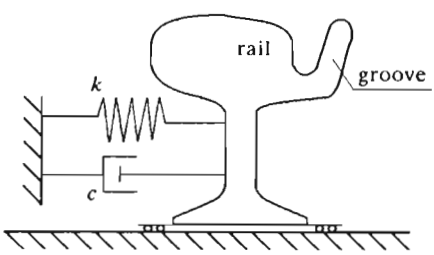

Fig. 7. Rail with a groove moving laterally

The force working on the flange, as well as the force at the main contact point, have two components:

1. Normal component – resulting from the rigidity of the wheel-rail arrangement

2. Tangent component due to the friction between the wheel flange and the head or groove of the rail.

To evaluate the flange contact normal force, a model of laterally moving rail was introduced. Then, a spring and dash-pot restriction on its motion was applied (cf Garg and Dukkipati, 1984), Fig7. For the tangent component, considering much lower values of forces at the flange contact point in comparison to the main point and considerable higher creeps at this point, a simpler friction model has been used. The following assumptions have been made:

1. In the area of contact between the flange and the rail that we consider, both the bodies are rigid and then the point contact occurs
2. Friction at the contact point is fully developed.

Then the flange force equals

$$F_t = \mu F_n \tag{2.7}$$

The friction force acts along this same line and has the opposite direction to the relative velocity of bodies.

3. Equations of dynamics

In contrast to a rather simple mechanical structure of the BW and BI bogies, the structure of BA bogie can be seen as a complex one. Moreover, because of big displacements of the elements the well-known small motion linearisation and simplification cannot be employed now. To deal with such a kind of structure, well developed multibody formalism has to be used (cf Maes et al., 1985). Another important aspect of the dynamical analysis is the wheel-rail stay-in-contact problem. The classical four degrees of freedom wheelset model (cf Garg and Dukkipati, 1984) cannot be employed now, due to the articulated nature of the BA bogie. Then the original concept of the wheel-rail contact treated as multibody structure constrains, introduced by Fisette and Samin (1992), has been employed. Finally, we have decided to generate the equations of motion on the basis of the "Recursive Newton/Euler Method", initially developed in robotics for solving the inverse problem of dynamics of a tree-like multibody system (cf Fisette et al., 1994).

We have assumed the following way of numbering the bodies in the system. The first element is treated as the reference element and identified with the system base. For an open system, that is the system that does not include a closed loop of bodies in its structure, individual elements (successors in the base) are numbered in the order in which they appear in the chain of elements. Individual joint (kinematic pair) receives a number which is identical to the body number for the body that follows it directly in the chain.

If the same numbering code is applied to a system having closed chains of elements, it becomes clear that there appears an element (see element A in Fig.8a) that is a predecessor of two (elements B and C in Fig.8a) or more elements having a common follower (element D in Fig.8a). Any element satisfying the conditions described above is called the loop origin. In the closed

loop case, to apply the numbering code mentioned above, it is necessary to make an imaginary cut in the closed chain structure. The "loop origin" element is then divided into two parts: the original part retaining all its physical properties and the fictions closing element which has only got kinematic properties, but which allows us to define the so-called, expanded graph structure.

The components of the model are rigid by definition. So the distribution of their masses is constant. Their mass parameters have the following symbols:

m_i – mass of the component element

$\boldsymbol{l}_{ii}$ – vector positioning the mass centre

$\boldsymbol{I}_{ii}$ – inertia tensor expressed in relation to the mass centre.

All of them are constant in the co-ordinate system fixed with the component.

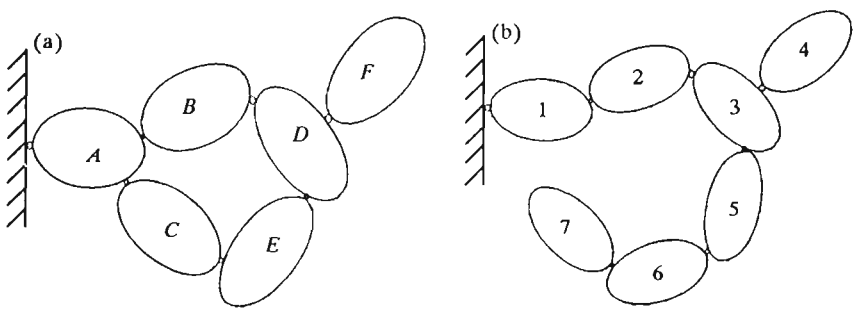

Fig. 8. System including a closed polygon of bodies (a) and the respective broadened structure with an example numbering (b)

3.1. Parameters describing the joint

While the model is in motion, the points connected with the joint belonging to different bodies can become closer or more distant (translational joints) and the co-ordinate systems (bases) fixed with the bodies attached by this joint can change their relative orientation (rotation joint). Relative motion of the joint final points can be described by a translation vector $\boldsymbol{z}^j$ and an orientation matrix $[A_{ij}]$, when

$$\boldsymbol{z}_j = [\hat{\boldsymbol{x}}_j][\boldsymbol{z}_j] \qquad [\hat{\boldsymbol{x}}_j] = [A_{ij}][\hat{\boldsymbol{x}}_i] \tag{3.1}$$

where

$[\hat{\boldsymbol{x}}_i]$ – column matrix constructed of the co-ordinate system unit vectors (versors) number i

$[\boldsymbol{z}_j]$ – column matrix of the co-ordinates of vector $\boldsymbol{z}_j$ expressed in the base $[\hat{\boldsymbol{x}}_j]$

$[A_{ij}]$ – orientation matrix, transforming the base $[\hat{\boldsymbol{x}}_i]$ into base $[\hat{\boldsymbol{x}}_j]$.

Matrices of coefficients $[A_{ij}]$ and $[\boldsymbol{z}_j]$ can be assessed basing on the displacement in the joint. Displacements in the joint will be generally treated as generalised co-ordinates q_j.

3.2. Equations of kinematics

Location of a component in the base co-ordinate system is defined, when we know:

1. The centre of mass position vector $\boldsymbol{x}_j$
2. Orientation of the body j fixed frame base $[\hat{\boldsymbol{x}}_j]$, with respect to the reference base

$$\boldsymbol{x}_j = \sum_{i=1}^{i\leq j} \boldsymbol{z}_i + \boldsymbol{l}_{ij} \qquad [A_j] = \prod_{i=1}^{i\leq j} [A_{ji}] \tag{3.2}$$

Given the location of bodies we can calculate their speeds

$$\dot{\boldsymbol{x}}_j = \sum_{i=1}^{i\leq j} \left(\dot{z}_i \boldsymbol{a}_i + \boldsymbol{\omega}_i \times (\boldsymbol{z}_i + \boldsymbol{l}_{ij}) \right) \qquad \boldsymbol{\omega}_j = \sum_{i=1}^{i\leq j} \dot{\theta}_i \boldsymbol{a}_i \tag{3.3}$$

and accelerations

$$\ddot{\boldsymbol{x}}_j = \sum_{i=1}^{i\leq j} (\ddot{\boldsymbol{z}}_i + \boldsymbol{l}_{ij}) \qquad \dot{\boldsymbol{\omega}}_j = \sum_{i=1}^{i\leq j} \ddot{\theta}_i \boldsymbol{a}_i + \boldsymbol{\omega}_{i-1} \times \dot{\theta}_i \boldsymbol{a}_i \tag{3.4}$$

where

$$\begin{aligned} \ddot{\boldsymbol{z}}_i &= \ddot{z}_i \boldsymbol{a}_i + \dot{\boldsymbol{\omega}}_i \times z_i \boldsymbol{a}_i + 2\boldsymbol{\omega}_i \times \dot{z}_i \boldsymbol{a}_i + \boldsymbol{\omega}_i \times \boldsymbol{\omega}_i \times z_i \boldsymbol{a}_i \\ \ddot{\boldsymbol{l}}_{ij} &= \dot{\boldsymbol{\omega}}_i \times \boldsymbol{l}_{ij} + \boldsymbol{\omega}_i \times \boldsymbol{\omega}_i \times \boldsymbol{l}_{ij} \end{aligned} \tag{3.5}$$

and $(i-1)$ stands for the body that directly precedes the body i.

The kinematic analysis is additionally provided with the equations of constrains which were removed from the system while constructing an expanded structure. In the program, two kinds of constrains have been examined. For the classical constrains, both the source and closing bodies must have the same position of the mass centre and identical base orientation. For the wheel-rail contact constrains, a full description of the constrain equation can be found in Fisette and Samin (1992).

3.3. Equations of dynamics

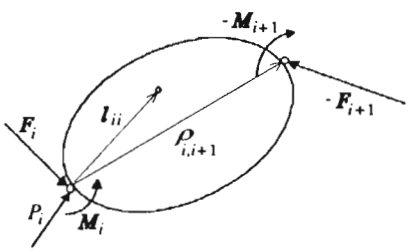

Fig. 9. Forces and force moments acting on body i

Using Newton's 2nd Law of Motion we can write (Fig.9)

$$\boldsymbol{F}_i = \boldsymbol{F}_{i+1}^{\Sigma} + m_i(\ddot{\boldsymbol{x}}_{pi}^{i} - \boldsymbol{g} + \dot{\boldsymbol{\omega}}_i \times \boldsymbol{l}_{ii} + \boldsymbol{\omega}_i \times \boldsymbol{\omega}_i \times \boldsymbol{l}_{ii}) \tag{3.6}$$

$$\boldsymbol{M}_i = \boldsymbol{M}_{i+1}^{\Sigma} + \boldsymbol{l}_{ii} \times \boldsymbol{F}_i + [(\boldsymbol{\rho}_{i,i+1} - \boldsymbol{l}_{ii}) \times \boldsymbol{F}_{i+1}]^{\Sigma} + \boldsymbol{I}_i\dot{\boldsymbol{\omega}}_i + \boldsymbol{\omega}_i \times \boldsymbol{I}_i\boldsymbol{\omega}_i \tag{3.7}$$

where

$\boldsymbol{F}_{i+1}^{\Sigma}$ – resultant of all forces acting in the joints which in the chains of bodies appear right after the body bearing the number i

$\boldsymbol{M}_{i+1}^{\Sigma}$ – resultant moment of all moments appearing in the joints which in the chains of bodies appear right after the body bearing the number i

$[(\boldsymbol{\rho}_{i,i+1} - \boldsymbol{l}_{ii}) \times \boldsymbol{F}_{i+1}]^{\Sigma}$ – sum of vector ratios $(\boldsymbol{\rho}_{i,i+1} - \boldsymbol{l}_{ii}) \times \boldsymbol{F}_{i+1}$ counted for all forces acting in the joints appearing in the body chains right after the body bearing the number i.

For the analysed system we can determine and control:

a) For a rotation joint – projection of the force moment vector acting in the joint on the axis of the joint

b) For a translation joint – projection of the force vector acting in the joint on the motion direction axis.

Because the above quantities can be controlled by us, these data are the function of springs deformations, dampers velocities, driving force and external forces applied to the joint.

The equation of the analysed extended body system dynamics takes the following form

$$P_i = \begin{cases} \boldsymbol{M}_i \cdot \boldsymbol{a}_i & \text{for a rotation joint} \\ \boldsymbol{F}_i \cdot \boldsymbol{a}_i & \text{for a translation joint} \end{cases} \tag{3.8}$$

After regrouping the expressions appearing with derivations of the joint displacements, these equations will assume the following form

$$\mathbf{M}(\mathbf{q}, t)\ddot{\mathbf{q}} = \mathbf{Q}(\dot{\mathbf{q}}, \mathbf{q}, t) \tag{3.9}$$

where

$\mathbf{q}$ – column matrix of generalised variables, describing configurations of all the bodies being parts of that expanded system

$\mathbf{M}(\mathbf{q}, t)$ – mass matrix (the elements of this matrix depend on the components of a $\mathbf{q}$ vector and time t)

$\mathbf{Q}(\dot{\mathbf{q}}, \mathbf{q}, t)$ – column matrix of generalised forces (not including the effects produced by the constrains).

3.4. Reduction of dependent variables

The constrains introduced into the system can be shown in the matrix form

$$\Phi(\mathbf{q}, t) = \mathbf{0} \tag{3.10}$$

where $\Phi(\mathbf{q}, t)$ is the column matrix of constrain functions.

In all the systems we can meet in practice the constrain functions are constant and have derivatives of the second order.

Making the additional assumption that the equations in the system (3.10) are independent, there is the Jacobian

$$\mathbf{Q}_q \equiv \left[\frac{\partial \Phi_i}{\partial q_i}\right] \tag{3.11}$$

which is a matrix having dimensions $n \times m$, and the order m.

Bearing the above assumptions in mind, on the basis of Lagrange's equations of the 1st kind, the dynamic equation for a joint system can be written as

$$\mathbf{M}(\mathbf{q},t)\ddot{\mathbf{q}} + [\mathbf{Q}_q(\mathbf{q},t)]^{\mathsf{T}}\boldsymbol{\lambda} = \mathbf{Q}(\dot{\mathbf{q}},\mathbf{q},t) \tag{3.12}$$

where $\boldsymbol{\lambda}$ is the Lagrange multiplies vector.

Now, separating the dependent and independent variables in Eqs (3.10) and (3.12), we have

$$\mathbf{M}^{uu}\ddot{\mathbf{u}} + \mathbf{M}^{uv}\ddot{\mathbf{v}} + \boldsymbol{\Phi}_u^{\mathsf{T}}\boldsymbol{\lambda} = \mathbf{Q}^u \tag{3.13}$$

$$\mathbf{M}^{vu}\ddot{\mathbf{u}} + \mathbf{M}^{vv}\ddot{\mathbf{v}} + \boldsymbol{\Phi}_v^{\mathsf{T}}\boldsymbol{\lambda} = \mathbf{Q}^v \tag{3.14}$$

$$\boldsymbol{\Phi}_u\ddot{\mathbf{u}} + \boldsymbol{\Phi}_v\ddot{\mathbf{v}} = -(\boldsymbol{\Phi}_q\dot{\mathbf{q}})_q\dot{\mathbf{q}} - \boldsymbol{\Phi}_{qt}\dot{\mathbf{q}} - \boldsymbol{\Phi}_{tt} \equiv \gamma \tag{3.15}$$

$$\boldsymbol{\Phi}_u\dot{\mathbf{u}} + \boldsymbol{\Phi}_v\dot{\mathbf{v}} = -\boldsymbol{\Phi}_t \equiv \upsilon \tag{3.16}$$

$$\mathbf{u} = \mathbf{h}(\mathbf{v},t) \tag{3.17}$$

where

- $\mathbf{u}$ – dependent variables coefficient vector
- $\mathbf{v}$ – independent variables coefficient vector
- $\mathbf{h}$ – set of functions of $\mathbf{v}$ vector of variable and time t which solves Eq (3.10).

Eqs (3.13) and (3.15) $\div$ (3.17) help us determine $\mathbf{u}$, $\dot{\mathbf{u}}$, $\ddot{\mathbf{u}}$ and $\boldsymbol{\lambda}$. Next, using these values in Eq (3.14) we will receive a dynamic equation for a system including closed loops of elements of the form

$$\tilde{\mathbf{M}}(\mathbf{v},t)\ddot{\mathbf{v}} = \tilde{\mathbf{Q}}(\dot{\mathbf{v}},\mathbf{v},t) \tag{3.18}$$

where

$$\tilde{\mathbf{M}} = \mathbf{M}^{vv} - \mathbf{M}^{vu}\boldsymbol{\Phi}_u^{-1}\boldsymbol{\Phi}_v - \boldsymbol{\Phi}_v^{\mathsf{T}}(\boldsymbol{\Phi}_u^{-1})^{\mathsf{T}}[\mathbf{M}_{uv} - \mathbf{M}^{uu}\boldsymbol{\Phi}_u^{-1}\boldsymbol{\Phi}_v] \tag{3.19}$$

$$\tilde{\mathbf{Q}} = \mathbf{Q}^v - \mathbf{M}^{vu}\boldsymbol{\Phi}_u^{-1}\gamma - \boldsymbol{\Phi}_v^{\mathsf{T}}(\boldsymbol{\Phi}_u^{-1})^{\mathsf{T}}[\mathbf{Q}^u - \mathbf{M}^{uu}\boldsymbol{\Phi}_u^{-1}\gamma] \tag{3.20}$$

Now, the system of equations obtained includes only independent variables and has the form identical with Eq (3.9) for the open loop. This system can be solved using any optional numeric algorithm for solving the system of 2nd degree differential equations. The received solutions show the trajectory of the model caused by the applied force or kinematic input.

4. Computer simulation

4.1. Conditions for computer simulation

The models described in this work have been used in computer simulation for various kinds of vehicles. The front coach based on a BW, BI or BA bogie has been analysed.

Table 1. Model parameters

	Bogie BW	Bogie BI	Bogie BA
Dimensions			
carbody length [m]	6.4	6.4	6.4
wheelbase [m]	1.7	1.7	1.7
track gauge [m]	1.435	1.435	1.435
wheel diameter [m]	0.64	0.64	0.64/0.395
Masses			
carbody [kg]	15323	15323	15323
bogie frame [kg]	2.462	2.464	2.096
wheel [kg]	–	260	260/80
wheelset	570	570	–
Secondary suspension stiffens			
K_{long} [10^6 N/m]	2 × 6.35	2 × 6.35	2 × 6.32
K_{lat} [10^6 N/m]	2 × 3.55	2 × 3.55	2 × 3.17
K_{vert} [10^6 N/m]	2 × 0.53	2 × 0.53	2 × 0.32
Secondary suspension dumping			
C_{long} [10^3 N/m]	–	–	–
C_{lat} [10^3 N/m]	55	55	33
C_{vert} [10^3 N/m]	2 × 25	2 × 25	2 × 27

Data used for simulation was chosen in such a way that it represents typical conditions of a tram bogie operation. So:

- Bogies with cylindrical wheels profile were analysed
- The wheels were equipped with flanges set with a 3.5 mm clearance relative to the head of the rail
- The flanges profile was set as conical with 1.3526 rad slope
- The rail profile was set as cylindrical with 0.2 m radius

- At the initial moment the tram was set on a straight part of track
- the initial velocity of the tram was 7 m/s
- Behaviour of the tram entering a left-side curve was analysed
- The radius of curvature was 50 m
- The bogies wheels turn without any driving moment on them
- The rail-track inclination angle was set 0 rad
- Straight-curve transition time was set at about 1 s for front wheels.

4.2. Analysis of simulation results

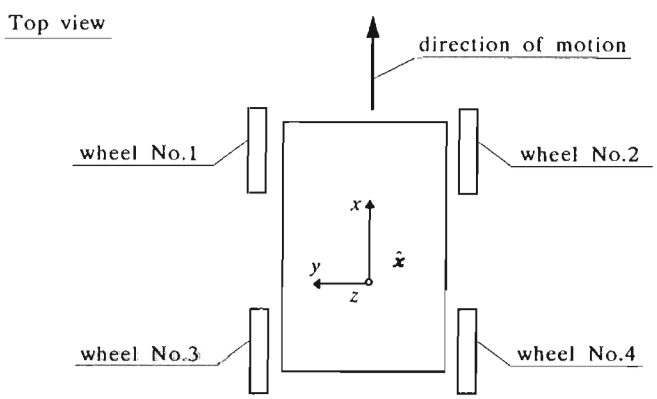

Fig. 10. The wheel numbering and frame orientation

The wheels force time histories for the all analysed structures have been presented on a common graph. For the components of forces which appear at the main point of contact, we have decided that their values are expressed in a frame which is fixed with the wheel. In the simulation initial configuration of these frames are collinear with the $\hat{x}$ frame (see Fig.10). For normal forces appearing flange contact point, we have decided to take them as positive.

4.2.1. Longitudinal force at the main contact point

As a result of the above analysis performed the following conclusions have been drawn:

- During the curvilinear motion the longitudinal force for the BW bogie is much greater than for the BI type (Fig.11). This is caused by a substantial difference in curve lengths covered by the wheels of the same axis. With the wheels connected to the axis in a rigid way, the difference in path can only be got rid of by a longitudinal slip.

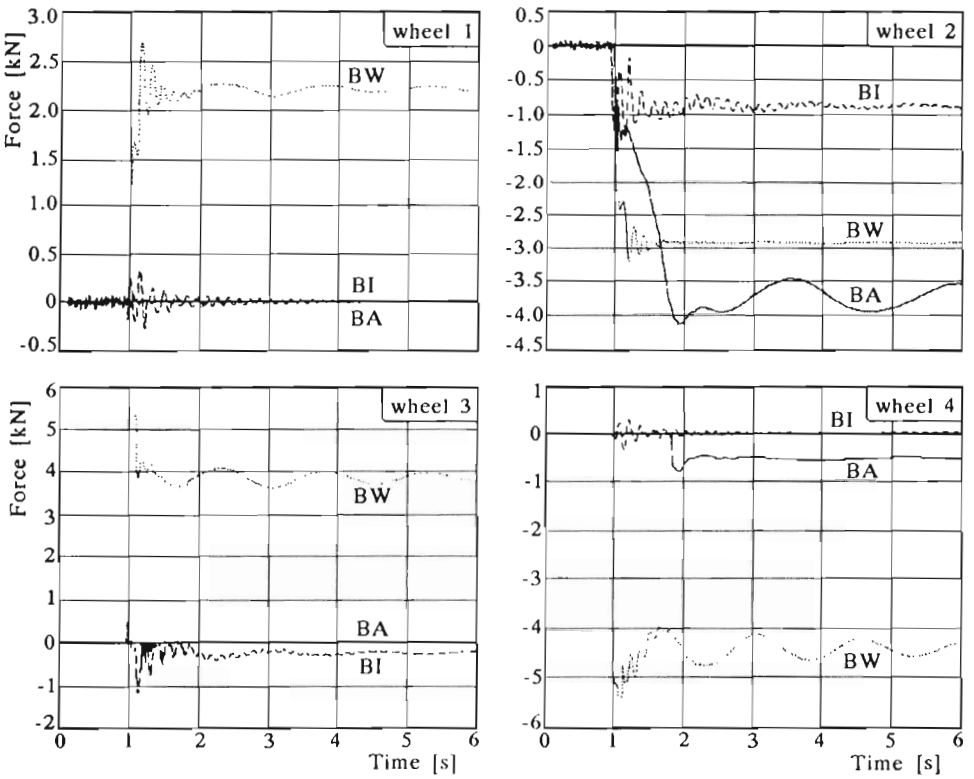

Fig. 11. Longitudinal creep force at the tread point of contact

- In the wheels working on the same BW bogie axis, the longitudinal forces act in the opposite direction. The moment about the rotation axis, caused by friction, is considerable. We have found out that because of a low acceleration resulting from the whole system dynamics, balancing the friction torque with the torque on the other wheel of the axis is indispensable.

- In the type BW bogie the longitudinal forces acting on the back wheels are greater than those on the front wheels. It is a consequence of the rotation about a vertical axis appearing in the original mounting (Fig.12a).

This rotation makes the angle of attack smaller and in the same way it makes smaller the transverse component of the friction force when the friction force is saturated.

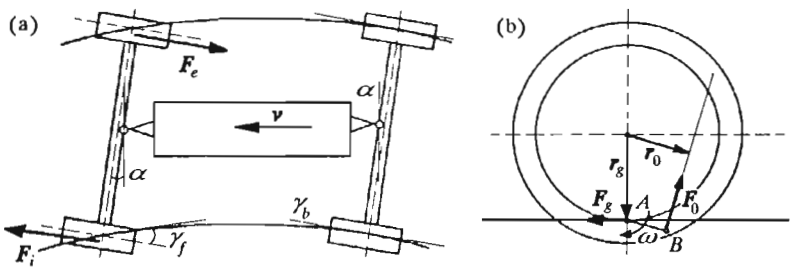

Fig. 12. Longitudinal creep forces acting on wheels of the BW bogie (a), creep forces configuration for a wheel having a contact point at the flange (b)

- For the type BI and BA bogies the longitudinal forces appear only with wheels having an additional contact point between the rail and the flange. The friction force at the contact point creates a torque about the axis of wheel rotation. Because of a low wheel acceleration resulting from the dynamics of the whole system, the equilibrium between the torque mentioned above and the torque created by the force in the main contact point is necessary (Fig.12b).

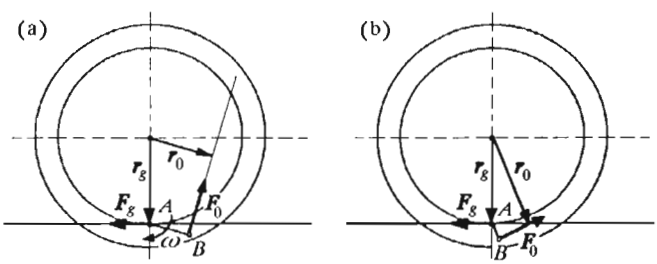

Fig. 13. Creep forces configuration for a wheel having a contact point at the flange: BW or BI bogie (a), BA bogie (b)

- For the wheels of the BA type bogie the longitudinal forces are greater than for the same wheels of the BI type bogie (Fig.11b). Because of the differences in the angles of attack, we can observe a different locations the contact point at the wheel flange (Fig.13). This difference results directly in higher values of the longitudinal forces for the BA bogie.

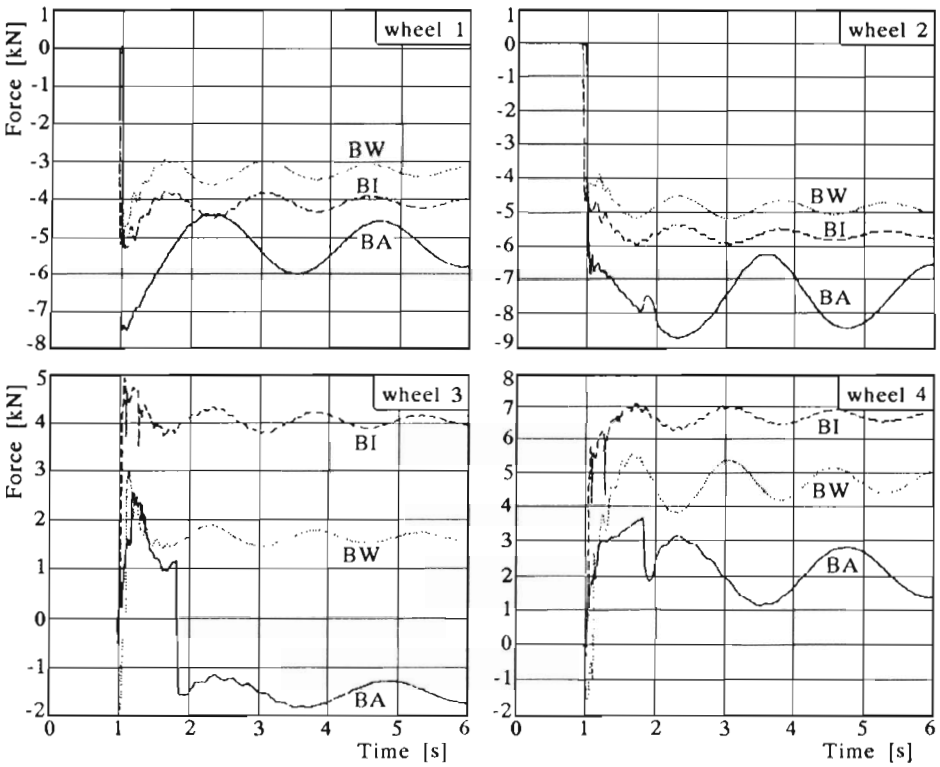

Fig. 14. Lateral creep force at the tread point of contact

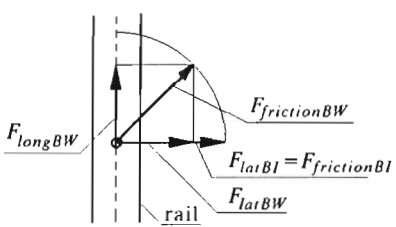

Fig. 15. Creep forces configuration at the tread point of contact

4.2.2. Lateral force at the main contact point

- The lateral forces for the wheels in the type BW bogie are smaller than the forces for the same wheels in the type BI bogie. They are marked in Fig.15 as F_{latBW} and F_{latBI}, respectively. We claim this is the effect of a greater value of F_{longBW} – the longitudinal component of the friction force $F_{frictionBW}$ which has been found fully saturated.

- The BA bogie is characterised by small lateral creep of a coach on a curve. For this bogie the angles of attack are big and, what follows, they produce big transverse creep in transient configurations between the bogie working on a straight rail and the bogie working on a curve.

- In spite of relatively small angles of attack of the wheels in the type BA bogie, the lateral friction forces at the main contact points of the front wheels have the biggest values of all the analysed types of bogies. A small angle of attack causes creepage comparable to the creepage limit (saturation limit). This limit was introduced to mark a point where the friction is modelled by the Culomb law (cf Eq (2.4)). Because of the construction asymmetry, the front wheels of the type BA bogie are additionally characterised by the greatest pressure forces operating between the wheel and the rail.

- For the BA bogie on a curve we can observe that lateral force on the back left wheel acts in has got the opposite direction to that on the back right wheel. The opposite directions of the force are the result of opposite signs of the attack angles of these wheels.

4.2.3. Normal force at the contact point between the flange and the rail

- In the right turn contact between the flange and the rail exists for the following wheels: front right and back left in the type BW and BI bogie, and front right and back right in the type BA bogie (Fig.16).

- For the BI bogie we can observe smaller normal forces at the contact point between the flange and the rail than for the wheels in the type BW bogie. This results from the two phenomena: a greater lateral friction component at the main contact point and a smaller torque about to the vertical axis, affected by longitudinal friction components at the main contact point.

  As we can see from the balance, the influence of smaller torque is more important than the influence of bigger lateral forces.

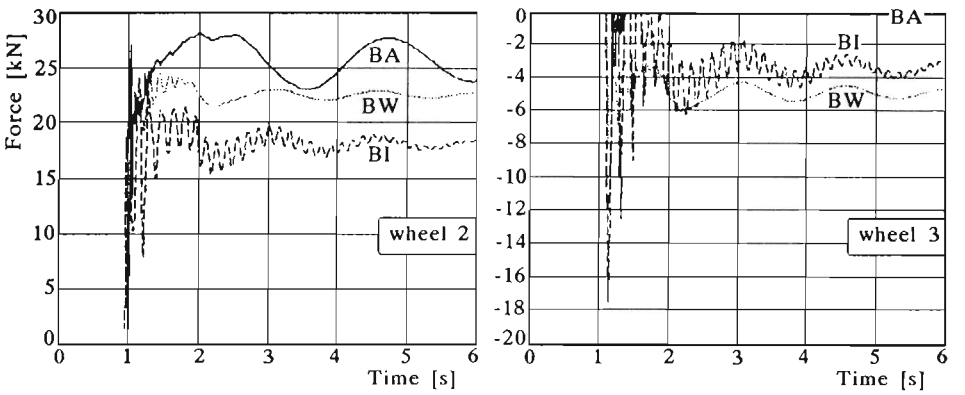

Fig. 16. Flange normal force

- The biggest pressure forces acting between the flange and the rail can be noticed for the front right wheel in the type BA bogie. It is caused by a non-uniform distribution of centrifugal force between the front and back wheels and the biggest of all the cases lateral friction force at the main contact point.

5. Conclusions

Analysing the interactions between the wheels and the rail for the presented above bogies we have drawn the following conclusions:

1. While negotiating the curve, relatively small dynamic effects appear in the analysed constructions and they show good stability during the on-curve motion on a perfect track. For this curve radius value negotiation there is no contact between the groove and the flange.

2. For type BA bogies, in spite of decreasing the angle of attack, it was not possible to lower considerably the interaction on the rail. The lateral creep observed in the simulation assumed values which are close to the creepage of the saturation limit. We can even notice some increase in the rail loading caused by asymmetry in distribution of the load between the front and back wheels.

3. In spite of the wheels in the type BI and BA bogies being mounted independently, the longitudinal friction components appear on the curves

at the main contact point. It results from the friction between the flange and the rail. A smaller angle of attack of that kind of wheels results additionally in greater longitudinal forces at the main contact point.

4. Smaller wheel-rail interactions types can be noticed for the type BI and the type BW bogie. However, for the BI bogie appear, weakly damped, high-frequency vibrations. Damping of those vibrations would require considerable alterations in the position of dampers in the bogie mounting.

Finally it should be mentioned that the interactions between the rail and the wheels should be studied more thoroughly. The analysed forces appearing at the same point act in opposite directions. The analysis should be supplemented by the global forces influence on the rail. The dissipated power analysis should be an interesting output too.

References

1. CARTER F.W., 1926, On the Action of Locomotive Driving Wheel, *Proc. R. Soc. London,* ser. A
2. FISETTE P., LIPIŃSKI K., SAMIN J.C., 1994, Symbolic Generation of Sub-Multibody Systems Applied to Urban Transportation Vehicle Dynamics, *CiSS – First Joint Conference of International Simulation,* ETH Zurich, Switzerland
3. FISETTE P., LIPIŃSKI K., SAMIN J.C., 1996, Dynamics Behaviour Comparison between Bogies: Rigid or Articulated Frame, Wheelset or Independent Wheels, *14th IAVSD Symposium on the Dynamics of Vehicles on Road and Track,* Ann Arbor, Michigan (USA), August 1995, edited at *Supplement to Vehicle System Dynamics*
4. FISETTE P., SAMIN J.C., 1991, Lateral Dynamics of a Light Railway Vehicle with Independent Wheels, *Proc. of the 12 IAVSD Symposium on the Dynamics of Vechicles an Road and Tracks,* Lion (France)
5. FISETTE P., SAMIN J.C., 1992, A New Wheel/Rail Contact Model for Independent Wheels, *Proc. of the Thire International Conference on Computer Aided Design, Manufacture and Operation in the Railway and other Advanced Mass Transit Systems "COMPRAIL 92",* Washington DC (USA)
6. GARG V.K., DUKKIPATI R.V., 1984, *Dynamics of Railway Vechicle systems,* Academic Press
7. HERTZ H., 1895, *Gasamelte Werke,* Vol.1, 155, Leipzig
8. KALKER J.J., 1967, On the Roling Contact of Two Elastic Bodies in the Pesence of Dry Friction, Ph.D. dissertation, Delft University of Technology, Delft, Netherlands

9. KALKER J.J., 1979, Survey of Wheel-Rail Rolling Contact Theory, *Vehicle Sys. Dynam.*, **8**, 317-358

10. KALKER J.J., 1990, *Three-Dimensional Elastic Bodies in Rolling Contact*, Kluwer Academic Publishers, Dordecht/Boston/London

11. KISILOWSKI J. ET AL., 1991, *Dynamika układu mechanicznego pojazd szynowy-tor*, PWN, Warszawa

12. MAES P., SAMIN J.C., SCHMIDT G., WILLEMS P.Y., 1985, Multibody Formalizm Applied to Non-Conventional Railway Systems, *Dynamics of Multibody Systems, IUTAM/IFToMM Symposium*, Udine (Italy), Septembre 1985, edited by G. Bianchi and W. Schiehlen, Springer-Verlag

13. WHITE R.C., LIMBERT D.A., HEDRICK J.K., COOPERRIDER N.K., 1978, Guideway-Suspension Tradeoffs in Rail Vehicle Systems, Raport DOT-OS-50107, U.S. Department of Transformation, Washincton, D.C.

Analiza porównawcza reakcji dynamicznych dla układów wózków tramwaju przy wchodzeniu w zakręt

Streszczenie

Metody stosowane w dynamice układów wielomasowych są powszechnie znanym i skutecznymi narzędziem badań dynamiki robotów i manipulatorów. Są one także wprowadzane do analizy dynamiki samochodów. Mimo to, dla metod tych poszukuje się nowych zastosowań. Komunikacja szynowa, a szczególnie tramwaje, będące popularnym środkiem miejskiego systemu komunikacyjnego, o złożonych konstrukcjach układów jezdnych nadają się doskonale do zastosowania tych narzędzi. Istniejąca literatura na temat dynamiki komunikacji szynowej w większości poświęcona jest pojazdom kolejowym. Niniejsza praca dotyczy analizy wózków jezdnych pojazdów szynowych pracujących w warunkach charakterystycznych dla komunikacji miejskiej. W porównaniu z koleją lub metrem, warunki pracy tramwajów posiadają znacznie więcej zewnętrznych ograniczeń. Przedstawiono wyniki symulacji komputerowej przeprowadzonej dla kilku rozwiązań układów jezdnych. Szczególną uwagę poświęcono wyborowi odpowiedniego modelu układu oraz modelu zjawisk zachodzących pomiędzy kołem i szyną. Analizowano zachowanie pojazdu na łuku o stosunkowo małym promieniu. Jako kryterium oceny wybrano siły reakcji powstające między kołem i szyną, a jej celem było znalezienie konstrukcji wywołującej najmniejsze obciążenia szyny. Wyniki symulacji komputerowej pozwoliły na zidentyfikowanie najważniejszych zjawisk wpływających na wielkość reakcji, a także oszacować je w różnych rozwiązaniach konstrukcyjnych wózków.

Manuscript received April 30, 1996; accepted for print May 13, 1997